We are IntechOpen, the world's leading publisher of Open Access books Built by scientists, for scientists

4,800
Open access books available

122,000
International authors and editors

135M
Downloads

Our authors are among the

154
Countries delivered to

TOP 1%
most cited scientists

12.2%
Contributors from top 500 universities

CLARIVATE ANALYTICS BOOK CITATION INDEX INDEXED

WEB OF SCIENCE™

Selection of our books indexed in the Book Citation Index in Web of Science™ Core Collection (BKCI)

Interested in publishing with us?
Contact book.department@intechopen.com

Numbers displayed above are based on latest data collected.
For more information visit www.intechopen.com

7

Tectonic Implications of Stratigraphy Architecture in Distal Part of Foreland Basin, Southwestern Taiwan

Jong-Chang Wu[1], Kenn-Ming Yang[2*],
Yi-Ru Chen[3] and Wen-Rong Chi[4]
[1]Exploration and Development Research Institute,
CPC Corporation, Taiwan, 1 Ta Yuan, Wen Sheng, Miaoli, 36010
[2,3,4]Department of Earth Sciences, National Cheng Kung University,
1 University Road, Tainan, 70101
Taiwan

1. Introduction

A foreland basin system with its asymmetric basin geometry extends from the frontal areas of a mountain-building belt to the margin of craton and includes, as defined by DeCelles and Giles [1], wedge-top, foreland basin, forebulge and backbulge. Foreland basins have been well modeled based on the concept of flexed lithosphere under tectonic loading of thrust sheets and sediments deposited into the basin [2, 3, 4]. Rapid subsidence in a ancient foreland basin and the uplifted forebulge at its distal part has been viewed as the result of tectonic loading due to active thrust sheet emplacement [5, 6, 7, 8]. Corresponding to each episodic thrust belt advancement, a coarsening-upward clastic wedge would form and prograde into the newly subsided foreland basin [9, 10, 11].

Characteristics of sedimentary sequences in a foreland basin are, thus, related to dynamic and kinematic modes of orogen-foreland basin evolution. Inversely, such characteristics can be used to investigate tectonic motion of the adjacent orogen [12, 13]. Different models for the development of a foreland basin predict distinct stratigraphy architecture across the basin. An elastic plate model predicts that the asymmetric foreland basin with the uplifted forebulge would migrate toward the craton as the rising orogen advances [14, 15, 16] and that the continuous migration of the orogen-foreland basin pair would leave a regional unconformity in the basin, which is younger toward the craton [17, 18]. The strata sequences overlying and onlapping at the unconformity have been viewed as the initial deposits of the foreland basin development [19, 20, 21, 22, 23]. The elastic model can be applied to infer the scale of erosion at the forebulge unconformity and the rate of strata onlapping across the unconformity under the conditions of variable crustal rigidity and variable migration rate of the orogenic wedge [22].

If a visco-elastic model is applied, the stress imposed on a loaded lithosphere would be relaxed and the foreland basin would become narrower and deeper with the forebulge migrating

* Corresponding Author

toward the orogen [2]. This would cause lithofacies belts to migrate back-and-forth between the mountain-building belt and craton and form a more complicated stratigraphic architecture at the basin and superimposed unconformities at the distal part of the basin [24, 25].

In many studies of foreland basin, the addressed deflexed plates are characterized by continental crust with heterogeneous mechanical property; the heterogeneity is manifested by a torn plate as the base of a foreland basin [26] or by lateral variation in crustal rigidity [27, 28, 29, 30]. More importantly, the mechanical heterogeneity is due to the fact that the predecessor of a peripheral foreland basin is a rifted continental margin with large-scaled normal faults distributed within the stretched continental crust and, for such reason, the location of foreland basin would migrate from the most stretched crust with the least rigidity to a complete nonstretched crust [31, 32, 33]. Therefore, an initially narrow-deep foreland basin would evolve into a wide-shallow one. In addition, pre-existing and syntectonic normal faults would influence the development of foreland basin sequences and shape an atypical time-spatial distribution of lithofacies in the basin [22, 34, 35, 36, 37].

Before the 1990s in the last century, the proposed models for foreland basin sequences basically assume that a foreland basin is filled up with deposits right after it forms. Lately, time lag between erosion in the mountain side and deposition in the basin has been put into consideration when investigating and simulating a model of foreland basin sequences [38, 39, 40, 41, 42, 43]. In response to each episode of active thrust faulting, newly formed foreland basin by rapid subsidence would not be filled up with sediments in the early time; therefore, according to the theoretical model [4], the sediment-starved basin would be deep and narrow and accumulate deep water sediments in an "underfilled" state [39, 40, 41]. In the following stage, the orogenic wedge began to uplift and the consequential erosion provided the sediments to fill up the basin when the large-scale thrust faulting wane. From that moment, the basin gradually becomes widened and shallow and step into the "overfilled" state characterized by shallow water deposits [44]. Generally speaking, in response to each episode of large-scale thrust faulting in the orogenic belt, the subsidence rate in a basin, which is related to the rates of advancement of the front of orogenic belt and change of orogenic wedge morphology, the sediment supply rate and the global sea level change rate would all together affect the tectonostratigraphic architecture, time-spatial distribution of lithofacies and the superimposed unconformities in the basin [39, 40, 41, 42, 45, 46, 47, 48, 49]. Some models suggest that timing of rapid subsidence at different locations in a foreland basin has different tectonic implication [40, 41, 43].

In a young and on-going mountain building belt, such as that in Taiwan, the geological records in the foreland basin and fold-and-thrust belt are still well preserved and can be utilized to study the tectonostratigraphy problems and to test validity of different models for the problems. Taiwan is located on the convergent plate boundary between the Eurasian and Philippine Sea plates; its tectonic belts are aligned from east to west: the island arc in the Coastal Range, the suture zone along the Longitudinal Valley Fault Zone, the inner mountain-building belt of high-grade metamorphism in the Basement Complex, the outer mountain-building belt of low-grade metamorphism in the Backbone and Hsuehshan ranges, the imbricate fold-and-thrust belt in the Western Foothills, and the foreland basin (Figure 1, [50]). According to the model and definition of DeCelles and Giles [1], the coastal plain and its subsurface settings of southwestern Taiwan has been located in the distal part and the adjacent forebulge of the foreland basin system since the Late Neogene [23, 51, 52, 53, 50]. The present day forebulge is located on the central line of the Taiwan Strait [23, 51, 52]. Owing to the paragenetic relationship between the foreland basin and the adjacent

mountain belt, the stratal sequences, lithofacies and subsidence history of the basin, especially those in the distal part and the forebulge of the basin system, would not only record the evolutionary history of the basin itself but also provide the most crucial indicators to infer the kinematics of the mountain-building process.

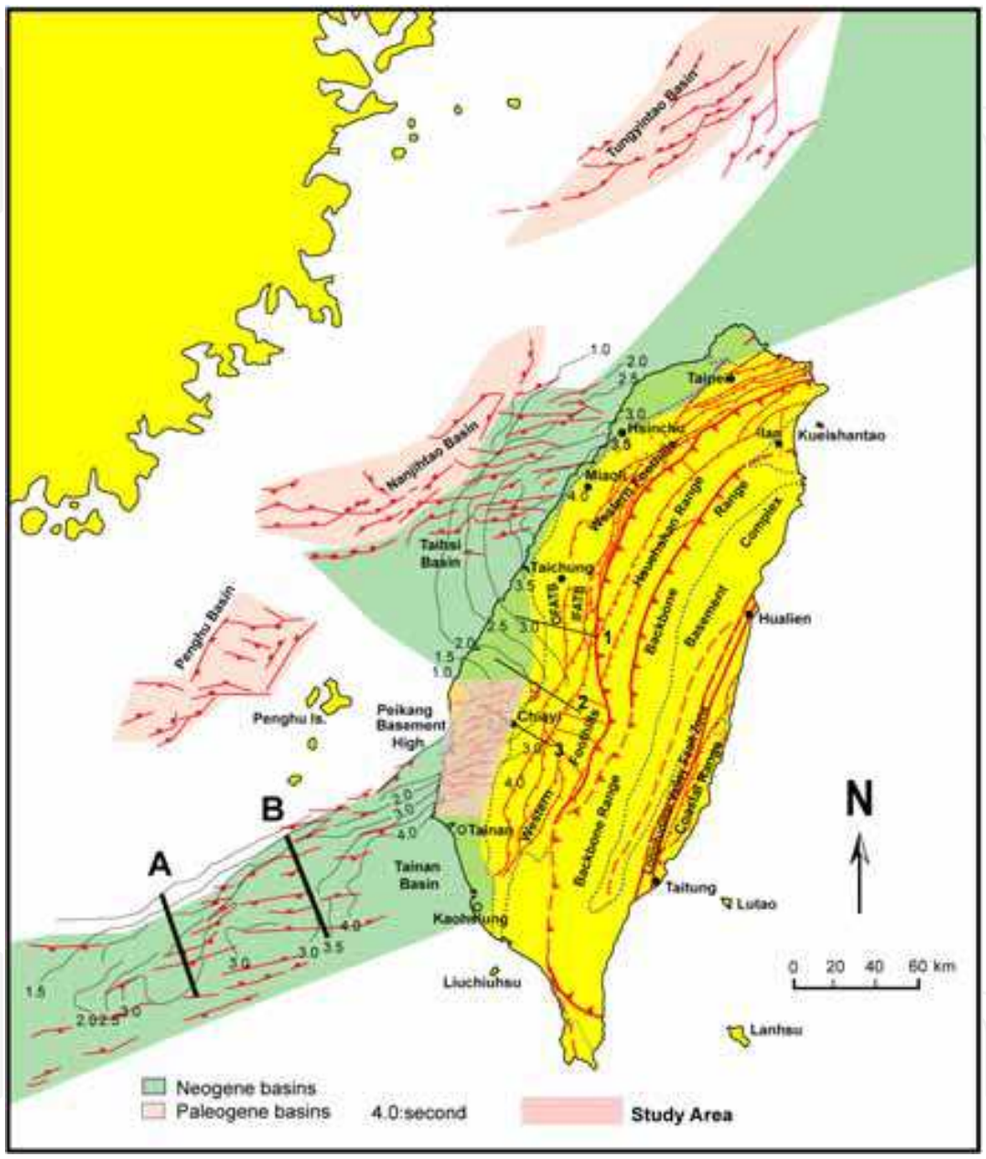

Fig. 1. Tectonic map of Taiwan and its adjacent areas. In the text of this article, the onshore foreland areas cover the alluvium and terrace gravel in the coastal plain, the outer fold-and-thrust belt (OFATB) and the inner fold-and-thrust belt (IFATB) in the Western Foothills. Note that, on this map, the Paleogene basin does not appear in the eastern part of the Taiwan Strait. This is because the Neogene settings are predominant in that area and almost overprint the Paleogene settings. WF, Western Foothills; HR, Hsuehshan Rang; BR, Backbone Range; BC, Basement Complex; LVFZ, Longitudinal Valley Fault Zone; CR, Coastal Range (From Yang et al. [50]). There are two rifted basins in the Neogene settings and the study area is in the northern margin of the southern basin.

The main purpose of this study is to integrate the well bore and seismic data to work on the analysis of subsidence history, stratal sequences and lithofacies in the distal part of the foreland basin in southwestern Taiwan (Figure 2). All the previous studies of the foreland basin in western Taiwan assumed that the mountain-building belt and foreland basin system have been continuously migrating westward to the craton since the initiation of the Taiwan orogeny [53, 54, 23, 50, 51]; they commonly regarded the deposits in the basin as a mega-sequence unit, based on which the time-spatial variation in lithofacies has been investigated and the geometry of the basin has been reconstructed. On the other hand, Yang et al. [55] analyzed the subsidence curves by Chi et al. [56] and pointed out that the tectonic development of the foreland basin and its counterpart in the mountain-building belt is episodic rather than continuous as proposed by Suppe [57]. Yang et al. [58] further proposed that the distal part of the foreland basin is characterized by superimposed unconformities in the subsurface and attributed the unconformities, with the bounded sequence units of third-order scale, and the following rapid subsidence to the episodic active thrust faulting in the mountain-building belt. The present article is the expansion of that proposed by Yang et al. [55, 58] and attempts to propose much more thorough descriptions and analysis of tectonostratigraphy in the distal part of the foreland basin in southwestern Taiwan. The first part of our works is to analyze in detail the subsidence curves in the distal part of the basin and to give a tectonic mode of epeirogenic movement in that area. We then propose two time-stratigraphy profiles based on the works of nanno-fossil age-dating from well bore data and seismic interpretation; we propose a more detailed and different tectonostratigraphic model from the previous studies. In the final part of this paper, we investigate the tectonic implications of the tectonostratigraphic model for the recent Taiwan orogeny.

2. Regional geology and previous studies

The Taiwan mountain-building belt is the result of the arc-continent collision between the Eurasia and Philippine Sea plates starting since the Pliocene (Figure 3; [59, 60, 61, 62]). During the orogeny, the westward vergent fault-and-thrust belt has also been propagating from the northeast toward the southwest owing to the oblique collision [63]. Age dating of nanno-fossil zones in the Coastal Range indicates that the age of the initial collision was 4 million years (My) [64]. Studies of sedimentary rock in the thrust belt show that the oldest sediments derived from the encroaching orogen are the Upper Pliocene [65]. However, Teng [66] suggested that the initial subsidence in the foreland basin due to tectonic loading of the growing orogenic wedge was in the Early Pliocene or at 5 Ma before present (bp). Teng [67] proposed that, according to the kinematic analysis of relative movement between the Eurasia and Philippine plates, the northern tip of the Philippine Sea plate started to collide with the boundary between continental and oceanic crusts in the Eurasian plate around 12 to 10 My bp and obducted over the passive margin of the Eurasian plate at 7 My bp. He also proposed that the mountain-building belt in northern Taiwan started to expose subaerially and propagate southward at 5 My and that a foreland basin in western Taiwan has developed since then. Huang et al. [68, 69] suggested that the timing of arc-continent collision should be at 6.5 My bp in northern Taiwan and 5 My bp in southern Taiwan.

Prior to the orogeny, the western Taiwan was located on the Eurasian passive continental margin (Figure 3) and had been went through two discernable major phases of Tertiary extensional tectonics (Sun, 1982; Yuan et al., 1989; Lin et al., 2003; Yang et al., 2006). The

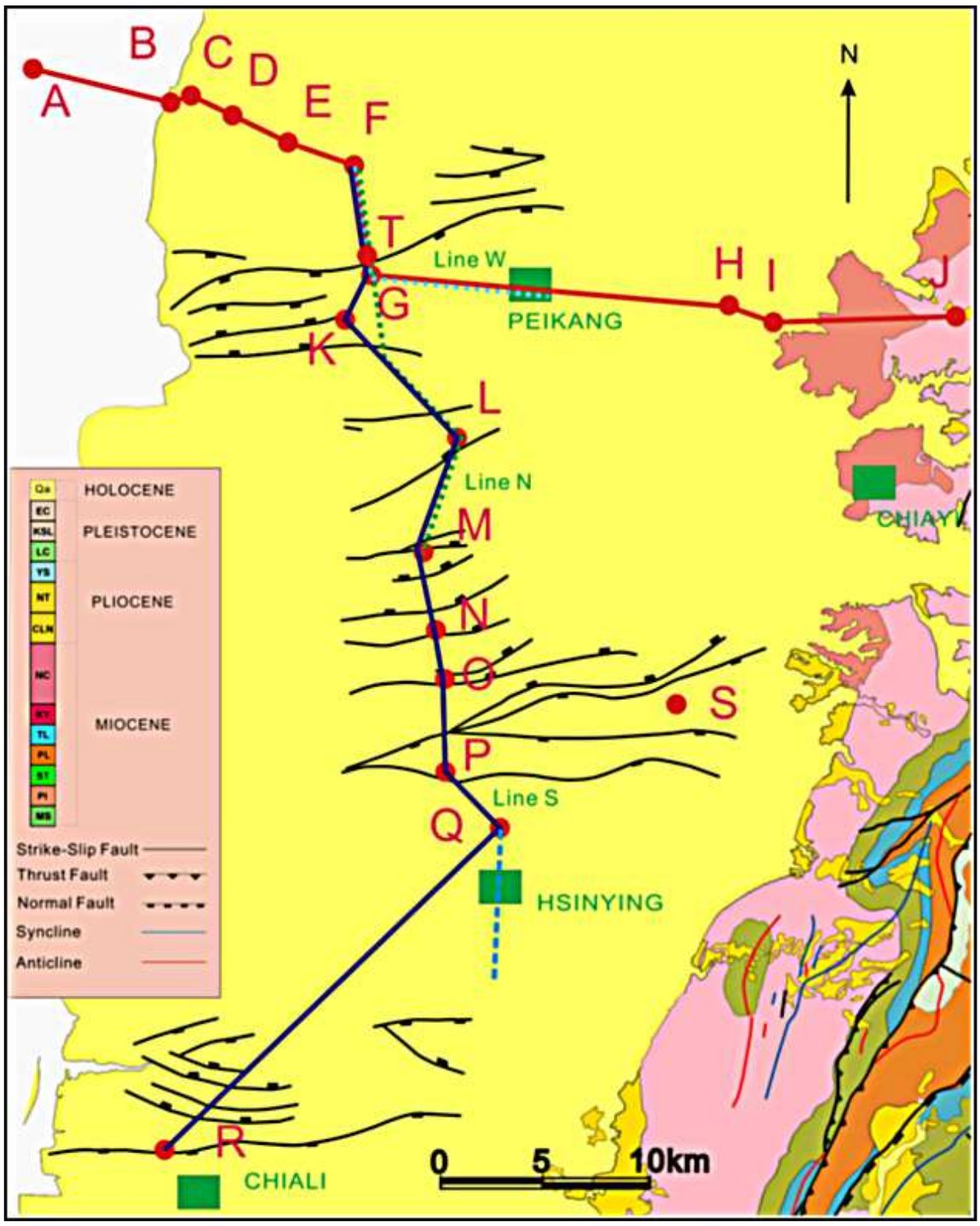

Fig. 2. Location map of well sites and seismic lines used for subsidence curve calculation and stratigraphy cross-section construction in this study. Locations of the east-west and north-south stratigraphy cross-sections are also shown in the map. The main subsurface structures in the study area are east-west striking normal faults. Part of foothills belt, which is characterized by fold and thrust structures, occurs to the east of the study area.

older phase primarily developed in the Paleogene period and ended in the Middle Oligocene [70, 71, 51, 52], forming a regional unconformity across the entire area of passive margin of southeastern China Mainland [70, 72]. However, the age of initiation of the post-rift sequences varies everywhere in the newly formed post-rift basin. In southwestern Taiwan, the age of the strata right overlying the regional unconformity is in NN1 zone [56]. The latest phase of the extensional tectonics initiated in the Middle to Late Miocene [73, 74, 70, 75 , 76, 77, 78, 71, 79, 51, 80] and formed two rifted basins separated by a basement high that stood nearly perpendicular to the front of thrust belt [80, 52]. The study area in this paper is located right on the northern margin of the southern rifted basins (Figure 1). The basin is composed of two opposite half-grabens (Figure 4), with its width increasing toward the northeast, indicating greater extension of the basin to the northeast (Figure 1; [80, 52]). The extensional tectonics is characterized by normal faults striking mainly east-west in the basin (Figures 1 and 2). The basin rifting has been propagating toward the southwest and the eastern part of the basin with greater extension now is buried beneath the fold-and-thrust belt [80]. The simple-shear model for the extension [81, 82] is applicable to interpreting the formation of the basin, because of not only the asymmetric feature across the basin but also its uplifting margins and subsiding center [70, 80]. This means that in the

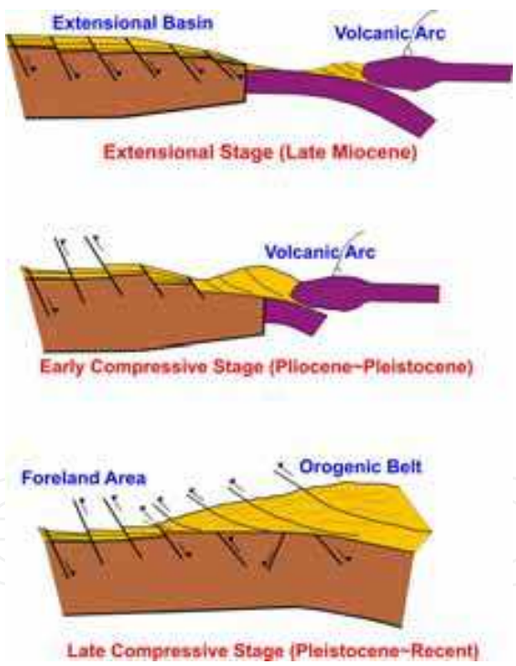

Fig. 3. Tectonic evolution of western Taiwan since the Late Miocene. Before the arc-continent collision, the passive margin of the Eurasia plate encountered the latest phase of extensional tectonics commencing from the Middle or Late Miocene. In the early stage of arc-continent collision, the preexisting normal faults that are close to the deformation front were reactivated while the extensional tectonics continued in the area to the west. In the latest stage, the inner part of the foothills belt have been dominated by low-angle thrusting while the reactivated normal faults and extensional tectonic stepped back to the foreland areas. More details about the structural setting in the foreland areas are given by Yang et al. [50].

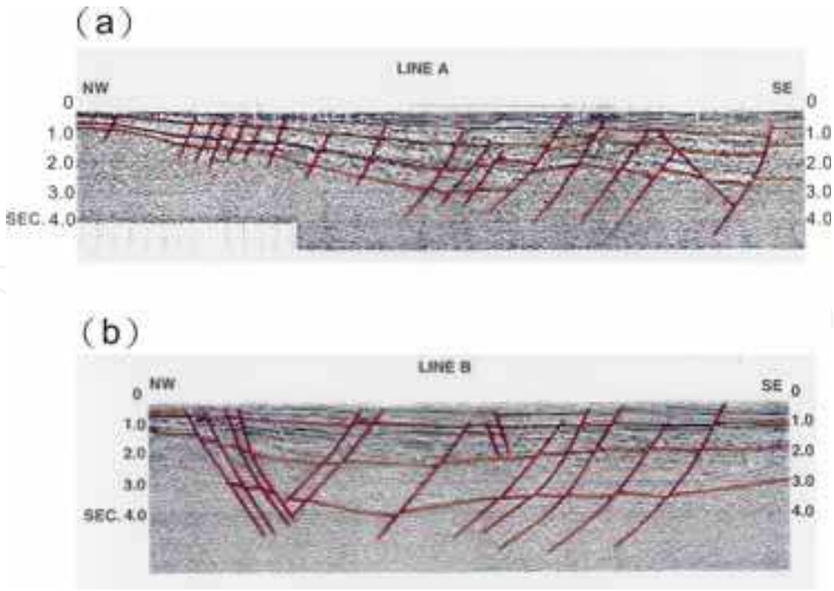

Fig. 4. Seismic sections showing half-grabens in the offshore area of southwestern Taiwan. The locations of the seismic lines are shown in Figure 1. The seismic lines run across the rifted basin, which formed during the latest phase of extensional tectonics. The rifted basin is composed of two opposed half-grabens with their widths widening to the east.

study area the foreland basin initially developed on the previously uplifted margin of the extensional basin [74, 70, 52]. Subsurface geology also indicates that normal faulting was still going on in the earlier stage of the foreland basin until the encroaching thrust sheets altered the local stress regime and caused the normal faulting to cease and step back cratonward [70, 52]. Although some studies attributed the latest stage of subsidence in the basin to the tectonic loading from the fold-and-thrust belt [83], so far no evidence has been found to indicate that the latest rifting and the recent collision were genetically related.

Referring to the geometric relationship between the passive continental margin and the thrust front, Suppe [57] assumed a constant migration rate for the westward advancement of the thrust belt and measured the rate of orogen growth and propagation along the passive continental margin. Based on the concept of critical taper of orogenic wedges, he also proposed that the mountain belt reached its today's elevation at about 3 My bp and that the cross-section width and area of the mountain range hadn't changed any longer since then [57].

The foreland areas in western Taiwan are equivalent to the areas covering the onshore fold-and-thrust belt (Western Foothills in Figure 1), the coastal plain outcropping with alluvial and terrace deposits, and the offshore Tungyintao, Nanjihtao, and Penghu basins developed in the Paleogene time (Figure 1). The fold-and-thrust belt is included as a part of the foreland area because its tectonic development has been strongly influenced by pre-existing normal faults. The coastal plain in southwestern Taiwan is located in front of the Taiwan mountain-building belt and the subsurface geological data from the coastal plain indicates that the thickness of upper Neogene, and depth of its correspondent sedimentary basin as well, increases dramatically toward the mountain-building belt to the east [70, 50, 52]. As for the offshore areas, structural cross sections [84, 85, 86, 49] through the Taiwan Strait show that the backbulge of DeCelles and Giles' [1] foreland basin system is almost equivalent to

the linear zone connecting the Tungyintao, Nanjihtao, and Penghu basins; therefore, the entire Taiwan Strait can be considered as the western part of the foreland.

Covey [53] was the first study on the foreland basin in western Taiwan; he suggested that the strata of the upper Pliocene to Recent in the foothills belt and coastal plain are the foreland basin sequences, which are characterized by the sedimentary facies that are shallower upward and orogenward and record the history of westward migration of the orogenic belt. Based on Suppe's [57] kinematic model of orogenic evolution, Covey [54] proposed that an underfilled foreland basin (corresponding to deeper water facies) in the early stage evolved into an overfilled one (corresponding to shallow water and continental facies) in the later stage and then entered a steady state in the following stage, i.e., the subsidence was balanced by the sediment accumulation in the basin. During cratonward migration of the orogenic belt the sequences in the proximal part of the basin were cannibalized into the mountain-building belt and a new space was created for sediment accumulation at the same time in the distal part of the basin. Thus, cross-secton width and area of the basinal profile remained constant through the time. This may be observed in the sedimentary sequences which monotonously consist of prograding shallow marine, deltaic and fluvial deposits. Covey [53] suggested that the initiation of the foreland basin was at 3 My bp. Based on the analysis of subsidence history in the onshore and offshore of western Taiwan, Chou et al. [88] comes to the same conclusion.

However, some studies suggested that the initiation of foreland basin development is earlier. Sedimentary facies in the foothills belt give some signatures of tectonic loading from the mountain-building belt to the east at 5 My bp [66]. In their model for calculating the rigidity of crust in western Taiwan, Shiao and Teng [85] first proposed that the boundary between the Miocene and Pliocene is the base of the foreland basin. Yu and Chou [23], using subsurface well bore and seismic data in the offshore of northwestern Taiwan, identified a regional unconformity at the boundary between the Miocene and Pliocene, on which the Pliocene strata onlapping westward to the craton. In other words, the time gap between the overlying and underlying strata of the unconformity increases to the craton. They suggested that the characters of the unconformity indicate the erosion and uplifting in a forebulge [22]; therefore, they regarded the regional unconformity as the base of the foreland basin. The unconformity in southwestern Taiwan that was previously interpreted as the initiation of the latest stage of extensional tectonics was also regarded as the southward extending part of that in northwestern Taiwan [23]. The interpretation about the age of foreland basin initiation was followed by Lin and Watts [50] and Lin et al. [51], by whom the age were more definitely assigned as 6.5 Ma.

Among the most recent studies, Simoes and Avouac [89], using the isopach maps of each sequence of the Neogene in the offshore and onshore of western Taiwan by Shaw [90], calculated the rate of westward migration of the orogenic belt since the foreland basin initiated at 6.5 My bp. Tensi et al. [91] also used Shaw's [90] isopach maps to infer the location of the forebulge during the past 12 My. Both studies pointed out that the inferred migration rate of the mountain-building belt and its associated foreland basin is not coincident with the rate, which is well constrained, of relative motion between the Eurasia and Philippine Sea plates today. The rate of southward migration of the mountain-building belt by Simoes and Avouac [89] is far less than that of relative motion between the plates and the inferred locations of the forebulge before 5 My bp by Tensi et al. [91] which implies an unreasonable width of the foreland basin.

3. Analysis of subsidence history

Subsidence curves (Figure 5) from the distal part of the foreland basin of southwestern Taiwan were calculated using stratigraphic thicknesses from well bore data. Subsidence histories were determined by "backstripping" methods [92, 93]. Decompaction constants used to restore stratal thicknesses are from the empirical porosity-vs.-depth curve compiled by Sclater and Christie [93]. The thickness ratio of sandstone to shale was measured to decide the decompaction constant for each sequence unit. To acquire the original strata thickness for constructing the burial history and the subsidence curves, we adopt the biostratigraphic units of nonno-fossil zone, which are regarded as more corresponding to the chronostratigraphic units, as an interval to be decompacted. The correlation between absolute ages and nanno-fossil zones was based on the works of [64] and Okada and Bukry [94].

In addition to the decompaction corrections, which gave the curve of "total subsidence", effect of sediment loading, depositional water depths and eustatic sea level fluctuation were also corrected in order to obtain the subsidence which is caused by tectonic loading. Traditionally, lithofacies and their corresponding depositional environments have been used to infer the local relative sea level. Nevertheless, the controlling factors for lithofacies change are more complicate. In order to avoid the controversies in interpreting the depositional water depths, statistic method based on foraminiferal fossil assemblages was adopted to evaluate the paleo-water depths for subsidence curve calculation. The range of eustatic sea level fluctuations during the Neogene was less than 250 meters [95]. This component of accommodation was not corrected from the subsidence curves shown below but does not affect the position of major inflection points of the curves.

All the subsidence curves were calculated based on the strata overlying the regional unconformity that represents the end of the Paleogene extensional tectonics and the beginning of the post-rift stage in the Neogene time. As mentioned above, the latest phase of extensional tectonics initiated in Middle to Late Miocene with uplifting in the basin margin and a remarkably localized unconformity occurs in the subsurface of coastal plain of southwestern Taiwan.

The correlative conformity from a continuous succession of well bore data can be viewed as the onset of uplifting and can be obtained by comparing the complete succession with the nearby eroded ones. The onset of uplifting is around 10 My bp for all the calculated subsidence curves. The magnitude of erosion by uplifting were estimated and used to calculate a complete subsidence history prior to the onset of the uplifting. To estimate the thickness of the eroded strata and their sedimentation rate, we used some wells such as J and R, which preserve the continuous succession in the localities closer to the basin center. The sedimentation rate then was multiplied with the time gap between the age of strata right underneath the unconformity and that of correlative conformity to obtain the thickness of eroded strata for each drilled well. It must be emphasized that, since the drilled wells with thickness of complete succession are located closer to the basin center, where is characterized by greater magnitude of subsidence, the thickness of eroded strata for the other drilled wells should be the maximum estimation.

The subsidence curves indicate a gradually decreasing rate of subsidence during the post-rift phase prior to the onset of uplifting. The uplifting then was followed by another phase of rapid subsidence. The onset age of the intial rapid subsidence varies in the study area, but in general it is stepwisely younging to the northwest (Figure 5), indicating a progressive onlapping of deposits at the unconformity. However, the variation in age of initial rapid

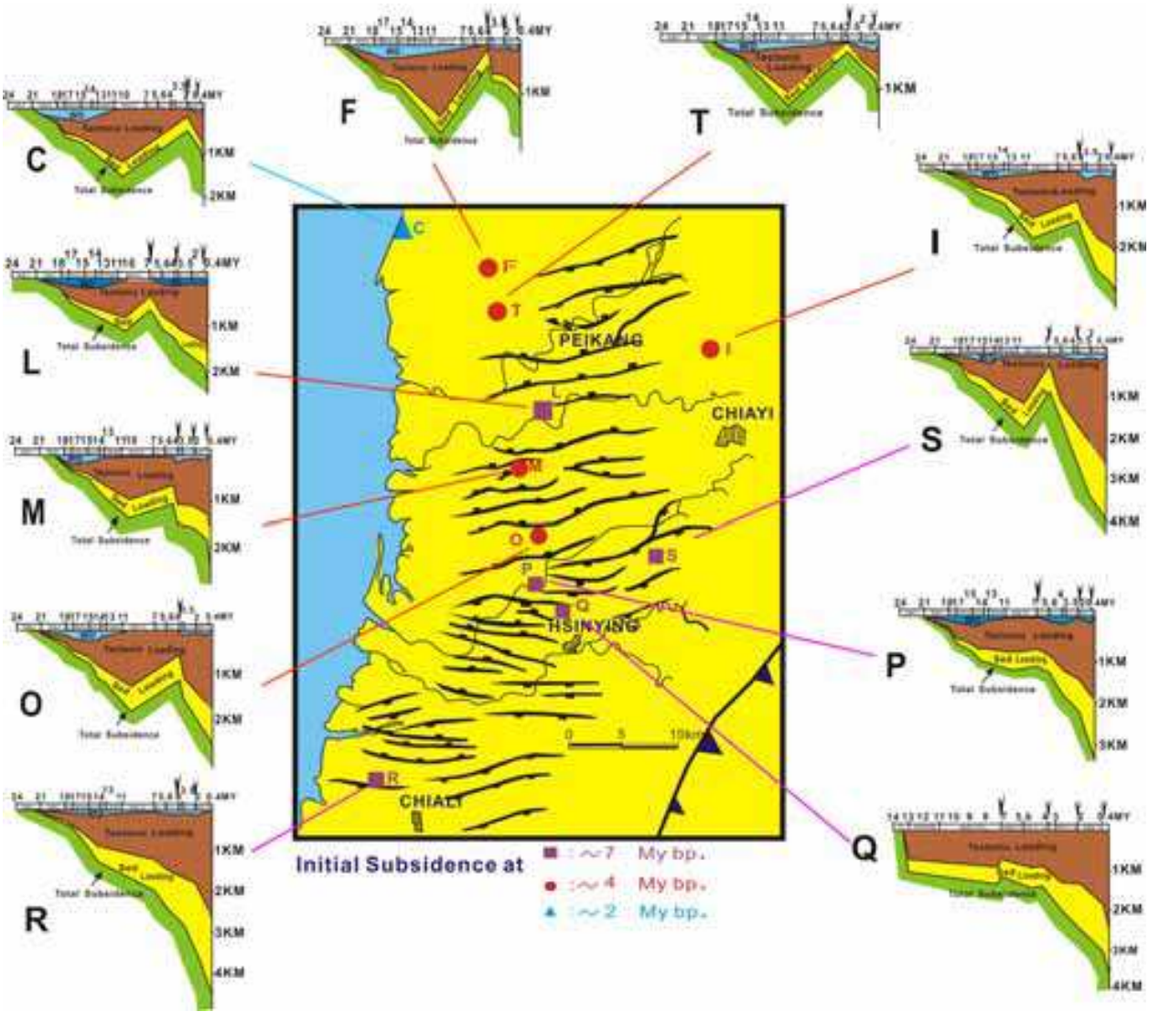

Fig. 5. Subsidence curves from drilled wells in the study area and location map of well sites with different ages of initial rapid subsidence. Arrow heads on each subsidence curve mark the ages of rapid subsidence initiation, which can be discerned as around 7, 5 to 4, 2 and 0.4 My. The well sites can be divided into three groups based on the age of initial rapid subsidence. Subsidence curves were modified from Chi et al. [56]. Detailed discussions of the subsidence curves are given in the text.

subsidence is not continuous across the entire study area; rather, the ages of onset of initial rapid subsidence can be discerned as around 7, 5 to 4, 2 and 0.4 My, although each age is within a small range of time. The well sites can be divided into three groups based on the age of initial rapid subsidence (Figure 5). In general, the well sites of younger ages of initial subsidence are located closer to the northwest. The first group of well sites with initial rapid subsidence onset at 7 My bp are located in the southeastern part of the study area. The subsidence curves show that rapid subsidence was followed by a period of slow subsidence, which in turn was followed by the next rapid subsidence with stepwise increasing rate (Figure 5). It is noticeable that even the subsidence curve from the drilled well of continuous succession shows the similar geometry of subsidence curve. The second group of well sites with initial rapid subsidence onset during 5 to 4 My bp are located to the northwest of the

first group. Although the age of rapid subsidence is younger, the subsidence curves show the same geometry. The third group, which is represented by only one well site with initial rapid subsidence starting at 2 My bp, located at the northwestern part of the study area. The subsidence curve shows a convex-upward geometry, indicating an increasing rate of subsidence.

Comparison among the four groups of subsidence curves indicates that those subsidence curves that mark the earlier initial rapid subsidence also record the younger phases of rapid subsidence (Figure 5). Therefore, the entire area in the distal part of the foreland basin in southwestern Taiwan had underwent four discernible episodic phases of rapid subsidence starting at 7, 5 to 4, 2, and 0.4 My bp. The time-spatial distribution of the onset ages of rapid subsidence indicates that the area affected by the tectonic loading, which is manifested by rapid subsidence, have been progressively expanding to the northwest. Among the first group of well sites, well G is an exception; it is located among the well sites of younger rapid subsidence. Its tectonic implications will be deciphered in the next section after we demonstrate the subsurface structural and stratigraphic features from seismic interpretation.

4. Time-stratigraphy architecture

The local exploration geologists who work on the subsurface geology in the coastal plain of southwestern Taiwan used to adopt the boundaries of lithostratigraphic unit when working on the stratigraphic correlation. The lithofacies identification for each litho-stratigraphy unit is based on that of type section occurring in the foothills belt. Using the boundaries of litho-stratigraphy units for stratigraphic correlation is applicable to the strata deposited in the Miocene, during which the subsidence was slow in comparison with that in the later foreland basin period (Figure 5) and eustatic sea level fluctuation overwhelmed tectonics in shaping the stratigraphic architecture. Under such condition, the boundaries of litho- and chronostratigraphic units are nearly parallel or even identical [75, 77]. However, the situation is different for the foreland basin sequences, of which lithofacies change dramatically from that occurs in the foothills belt to that in the subsurface in the coastal plain [53, 54]. The lateral lithofacies changes even appear in local area; biostratigraphic study results from the southern part of this study area by Wu et al. [96] indicate that the sedimentary cycles are not coincident to the eustatic sea level fluctuation and, instead, strongly affected by tectonics. The study of sedimentary environments of the section in the foothills belt also gives the same conclusion [97]. In order to accurately illustrate time-spatial distribution of strata in the distal part of the foreland basin, we used the top of nanno-fossil zones from the drilled wells as the time line to construct a time-stratigraphic cross-section across the study area. Previous studies [74, 53, 77, 78, 23, 52] have shown that the base of the latest rift settings, and the foreland basin as well, in southwestern Taiwan deepens from the basement high in the northwestern part of the study area to the east and south. We constructed both north-south and east-west lines of time-stratigraphy cross-section; the former could be used to investigate the effect of the normal faulting on the stratigraphic architecture while the later would illustrate a typical asymmetric stratigraphic profile across a foreland basin.

The line of east–west stratigraphy cross-section extends from the near shore area in the west to the area very close to the thrust front of the foothills belt in the east (Figure 2). The well sites are mostly located in the western and eastern parts of the line. The stratigraphic architecture in the middle part is mainly constrained by seismic interpretation, which will be

addressed below. The stratigraphy cross-section (Figure 6a) shows an eastward thickening succession, which is punctuated by two regional unconformities, which become conformities to the east. The localities of transition between the unconformities and their correlated conformities shift to the west. The time gap between the strata underlying and overlying the unconformities also increases to the west. Well J is at the eastern end of the line and its succession is continuous from the sequences of extensional basin to that of foreland basin. To its west, strata of NN11-13 onlap at the unconformity that is at the base of the foreland basin and pinch out at very short distance. In the middle part of the line the strata of NN11-13 appear again but terminate at a southeast-dipping normal fault that can be unequivocally interpreted on the seismic section line W (Figure 6b). The normal fault is the major boundary fault occurring along the northern margin of the latest extensional basin. Distribution of strata NN-14 continuously extends to the west until where they are truncated by another younger regional unconformity. The unconformity at the base of the strata NN 11-13 and 14 also merges with the younger unconformity to the west and forms another unconformity with large time gap between the underlying and overlying strata. Strata of NN 15-18 are truncated by the younger unconformity in the area between wells G and H; the stratigraphic architecture of transition between unconformity and the correlated conformity is constrained by the interpretation on seismic section line W (Figure 6b). Strata of N19 are ubiquitously overlying the younger unconformity and its correlated conformity across the entire cross-section. Comparing to entire foreland basin sequences, especially those between two unconformities and their correlated conformities, the eastward thickening of each unit of nanno-fossil zone, except strata of NN11, is not so remarkable. The most widespread units, NN14 and NN19, uniformly spread to the west where their thickness obviously decreases or they are truncated by the younger unconformity.

In order to illustrate the variation in stratal units across the boundary normal fault zone, part of the northern segment of north-south stratigraphy cross-section was designed to overlap with east-west cross-section (Figure 2). The stratigraphic architecture on north-south stratigraphy cross-section (Figure 7a) is similar to that on east-west cross-section; the foreland basin sequences thicken toward the basin center to the south and are truncated by two major regional unconformities, of which the spatial distribution of the younger one steps back to the north. Still, north-south cross-section shows some more complicated features of stratigraphic architecture, which are highly related to the normal faulting during the development of foreland basin. Thickening of the foreland basin sequences is not gradual but appears stepwise across several major normal faults of prominent displacement. In the northern part of the cross-section, stratal units of NN11-13 overlying the older unconformity are deposited in the downthrown side of the normal faults and separated from those deposited in the basin center where the units become conformable on the underlying strata. In the southern part of the cross-section, the strata of NN11, the oldest stratal unit overlying the older unconformity, are truncated by a local unconformity, which can be correlated to the stratal unit of NN12. Similarly, the stratal units of NN11-13, including the local unconformity between the units of NN11 and NN13, terminate at another major south-dipping normal fault. The existence of normal fault in shaping distribution of the stratal units of NN11-13 can be clearly illustrated by the interpretation on the seismic line N (Figure 7b). The boundary between the stratal units of NN11-13 and NN14, as shown on seismic section line N (Figure 7b), shows as an undulating feature, indicating erosion cutting down to the underlying strata. The scale of erosion is too significant

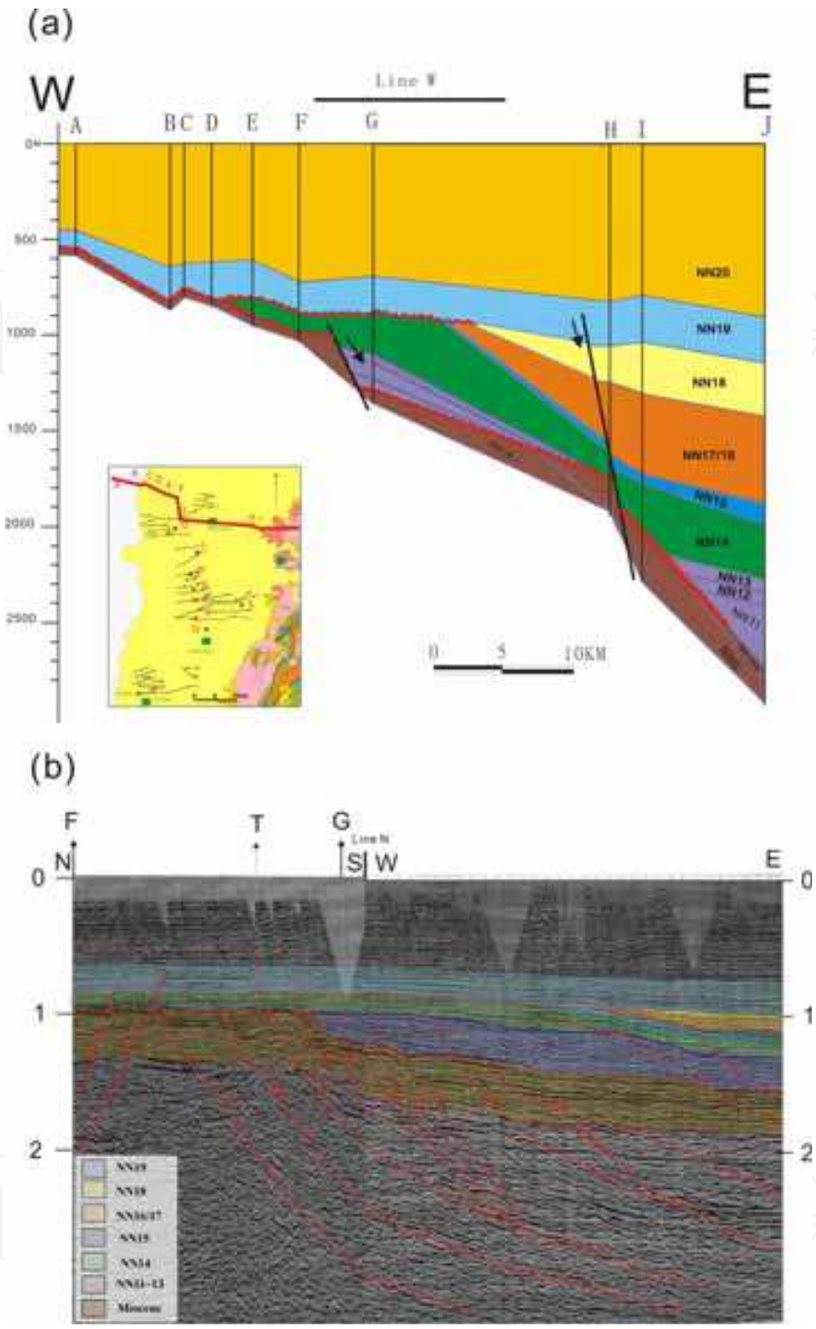

Fig. 6. Time-stratigraphic architecture of the foreland basin sequences shown by (a) east-west stratigraphy cross-section and (b) seismic line W for local stratigraphy constraint. The inset map shows location of the stratigraphy cross-section. The range of the seismic line is also marked on the stratigraphy cross-section. Although spatial distribution of strata is affected by normal faulting, the stratigraphic architecture illustrates westward younging stratigraphic settings, including the spatial distribution of the unconformities with their correlated conformities and the overlying strata. The normal fault that controls the deposition of localized strata of NN11-13 is constrained by the interpretation of the seismicc line W.

to be detected by nanno-fossil dating and, therefore, the corresponding unconformity does not appear on the stratigraphy cross-section. Nonetheless, its implication of sedimentation in the scheme of foreland basin will be addressed below. Localized distribution of the strata of NN15-17 underlying the younger unconformity is also shown on north-south stratigraphy cross- section (Figure 7a). Interpretation on the seismic section line N (Figure 7b) indicates that such distinct stratigraphic feature can be attributed to fault block tilting by normal faulting.

Wheeler diagrams (Figure 8) were constructed based on the stratigraphy cross-sections to illustrate time-spatial distribution of each nanno-fossil zone. On the east-west diagram (Figure 8a), the time gap of each regional unconformity increases to the west where the strata of NN19 directly overly the strata of NN6-7, the sequences prior to the foreland basin development. The diagram also shows that the basin margin, as defined by the boundary of eroded regime, has been migrating back-and-forth during the foreland basin development. The margin of the basin migrated toward the front of mountain-building belt to its farthest position during the NN11 zone and then started to retreat to the craton. The basin expanded cratonward rapidly to its maximum extent during the deposition of the strata of NN14. By the end of NN14, the basin margin migrated toward the front of mountain-building belt again and arrived at its easternmost position at NN8. Nonetheless, the easternmost position of the basin margin at this time is more cratonward than that at NN11, indicating cratonward shifting of the entire stratigraphic settings.

On the north-south diagram (Figure 8b), back-and-forth migration of basin margin still can be shown; however, the time-spatial distribution of strata of NN11-13 and NN15-18, which are coeval with the development of regional unconformities, are highly related to normal faulting of large displacement and occur in the downthrown side of the faults. Nonetheless, the ubiquitous unconformity-based stratal units, NN14 and NN19, basically are not affected by the normal faulting.

5. Discussions

Subsidence curves (Figure 5) and stratigraphy cross-sections (Figures 6, 7 and 8) in the study area give some important constraints for proposing any tectonostratigraphic models of foreland basin development in western Taiwan. In the sections below, we give some discussions regarding the controversies about several important related issues, including the initial time of foreland basin development, sedimentology of boundaries of third-order sequences and eustatic effects on the stratigraphy architecture. Once they are clarified, the tectonic implications of foreland basin sequences would be unraveled.

5.1 Onset time of foreland basin development

Rapid subsidence events starting at 5 to 4 and 2 My indicated by the subsidence curves can be well correlated to the unconformities and the overlying ubiquitous strata of NN14 and NN19. However, rapid subsidence event initiated at 7 My bp is not so well defined on the stratigraphy cross-sections (Figures 6, 7 and 8) because of onlapping of stratal units of NN11-13 at the unconformity occurs in the easternmost part of the study area. Since most part of the study area is located on the northern uplifting margin of the extensional basin, rapid subsidence following the uplifting at any places of the study area would be taken as the onset of tectonic loading during the foreland basin development. The onset age of the rapid subsidence at 7 My is very close to and might be correlated to that of the previously proposed initiation of the foreland basin in western Taiwan at the end of Miocene [85, 23, 49,

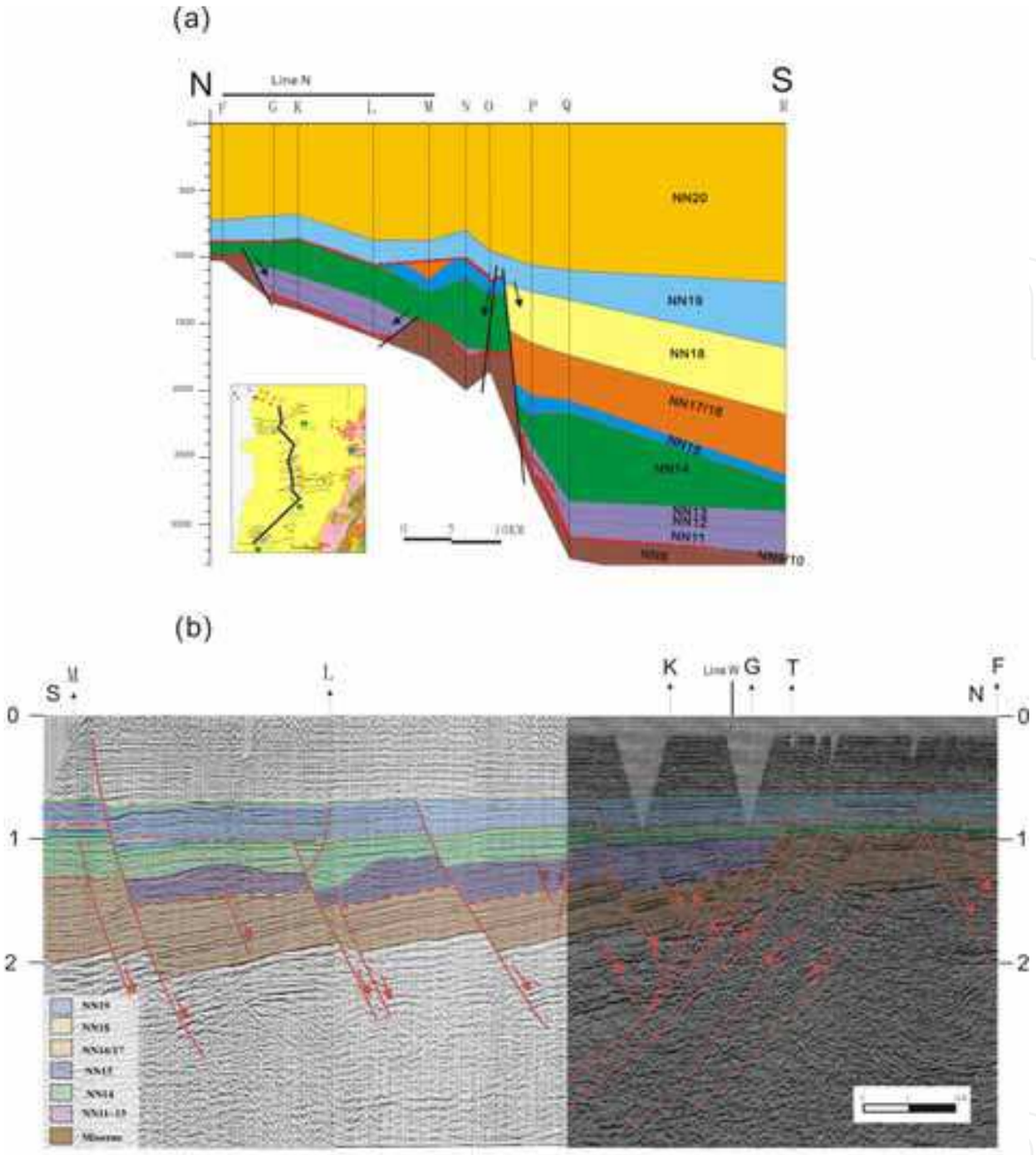

Fig. 7. Time-stratigraphic architecture of the foreland basin sequences shown by (a) north-south stratigraphy cross-section and (b) seismic line N for local stratigraphy constraint. The inset map shows location of the stratigraphy cross-section. The range of the seismic line is also marked on the stratigraphy cross-section. Spatial distribution of strata is highly affected by normal faulting; to the north of the normal fault located between wells O and P, the older unconformity is primarily at the base of strata of NN14 but is overlain by strata of NN11-13 in the downthrown side of normal fault of large displacement. To the south, foreland basin sequences are rather continuous, only disrupted by a local unconformity. Nonetheless, the stratigraphic architecture illustrates that stratigraphic settings, including the spatial distribution of the unconformities with their correlated conformities and the overlying strata, generally are younging to the north. Relationship of normal faulting with the irregular distribution of strata of NN11-13 can be illustrated on the interpreted seismic line N.

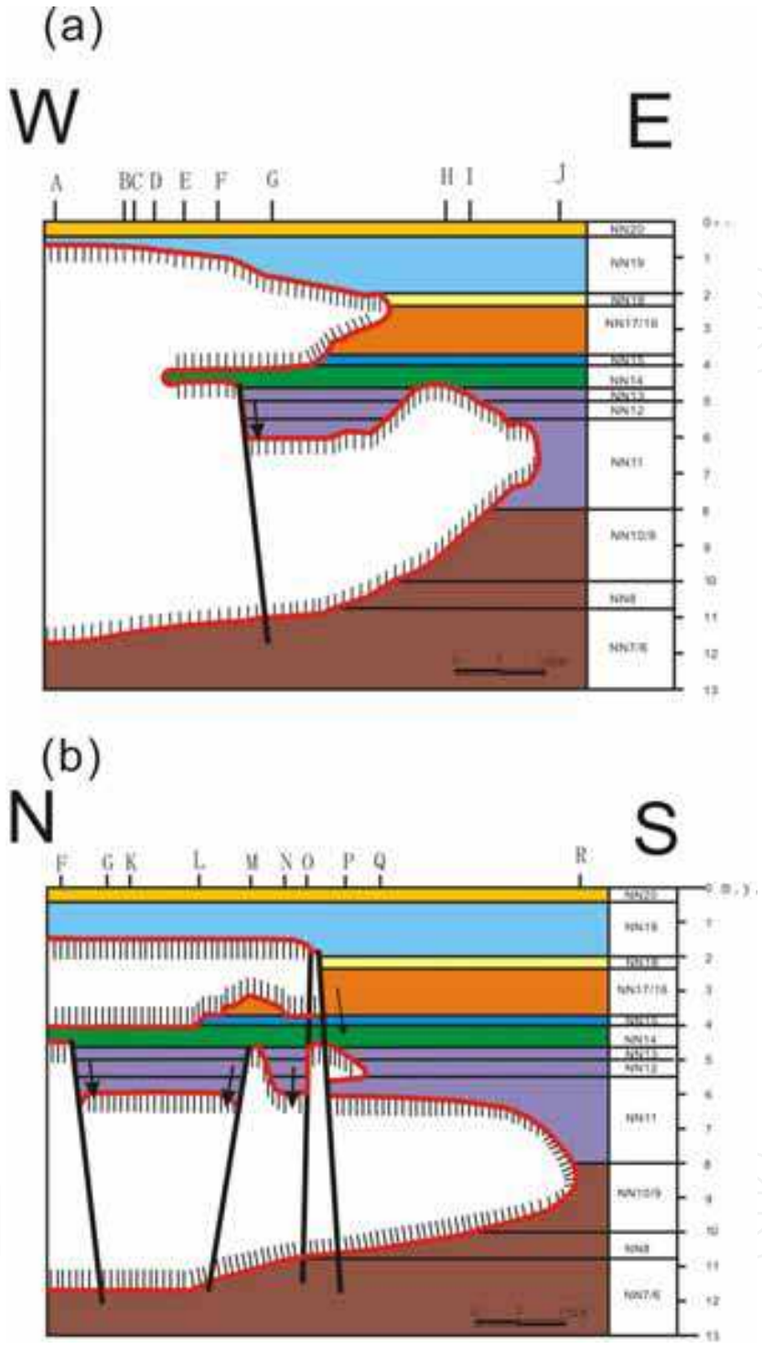

Fig. 8. Wheeler diagrams of (a) east-west and (b) north-south stratigraphy cross-sections, illustrating time-spatial distribution of the foreland basin sequences. On the east-west diagram, the time gap of each regional unconformity increases to the west where the strata of NN19 directly overly the strata of NN6-7. The basin margin, as defined by the boundary of eroded regime, has been migrating back-and-forth during the foreland basin development. On the north-south diagram, time-spatial distribution of strata of NN11-13 and NN15-18 are highly related to normal faulting and occur in the downthrown side of the faults.

50, 51, 89]. However, this contradicts some study results from northwestern Taiwan [66, 88], where the ages of initiation of foreland basin development have been dated younger than that in southwestern Taiwan. Considering the tectonic evolution of oblique collision for forming the mountain-building belt, the age of initiation of foreland basin development in the study area could only be younger than that in the northern areas. In addition, as pointed out by some previous studies [89, 91], the position of foreland basin margin in southwestern Taiwan at 6.5 My bp is not consistent with that deduced from the modern relative motion between the Eurasia and Philippine Sea plates. The occurrence of the stratal units of NN11-13 might give some answers to the controversy; the strata of the units, except that in the easternmost part of the study area where actually is in the basin center, were mainly accumulated in downthrown side of the major normal faults (Figures 6, 7 and 8), indicating that deposition of the units are highly related to the normal faulting. Therefore we suggest that the rapid subsidence onset at 7 My bp is the result of the normal faulting and rule out the possibility of foreland basin development onset at that time. We also suggest that the foreland basin had not commenced until the rapid subsidence onset at 5 to 4 My bp or the beginning of NN14.

5.2 Sedimentology of sequence boundaries

Subsidence curves (Figure 5) reveal four rapid subsidence events following uplifting and the causal unconformities. The resultant stratigraphic architecture can be divided into several sequence units of third-order scale bounded by the unconformities and their correlated conformities (Figures 6a and 7a). We demonstrate some prominent sedimentological features below to argue that the sequence boundaries are caused by or at least highly related to tectonic processes.

Well Q is located in the southern part of the study area. In terms of basin architecture, it is in the downthrown side of a major normal fault that is the demarcation between the uplifted margin and the basin center during the foreland basin development (Figures 2 and 7a). The subsurface succession from that well is continuous above the unconformity of 7 My bp between the stratal units of NN8 and NN11 (Figure 9). Sedimentary cycles of coarsening-upward can be identified as the sequence units of third-order scale and the sequence boundaries are at the unconformity-correlated conformities of 5 to 4, 2 and 0.2 My (Figure 9), distinctively. The characteristics of periodic coarsening upward sequences indicate a strong tectonic signature that can be comparable to other examples in some tectonically active belts [9, 10, 11]. The tectonic origin for the unconformities is also supported by the calculated magnitude of erosion of the unconformities in the Plio-Pleistocene [98], which scale is larger than that could be caused by eustatic sea level fall during the same period.

The well bore data was correlated to a seismic line tied to the well and the interpreted seismic profile shows that the sequence boundaries are characterized by prominent canyon morphology to the south of the well site (Figure 9). The largest scale of down-cutting morphology is the boundary at the base of the stratal units of NN19. The morphology of each submarine canyon has been studied and reconstructed in detail by Fuh et al.[99, 100] using a dense grid of seismic sections with some well bore data in the area between wells Q and R. The reconstructed morphology of submarine canyons shows that the regional trends of the axis of submarine canyons are parallel with that of the mountain-building belt, implying that the formation of the unconformities is related to the orogeny. Their studies also show that the submarine canyons gradually developed southward, consistent with the general trend of southward propagation of the mountain-building belt, but bounced back to

the north relative to the preceding one when the most prominent canyon was developing at the base of NN19 [99]. Such back-and-forth pattern of submarine canyon migration is correlated to that shown on the stratigraphy cross-sections (Figures 6a and 7a) to the north.

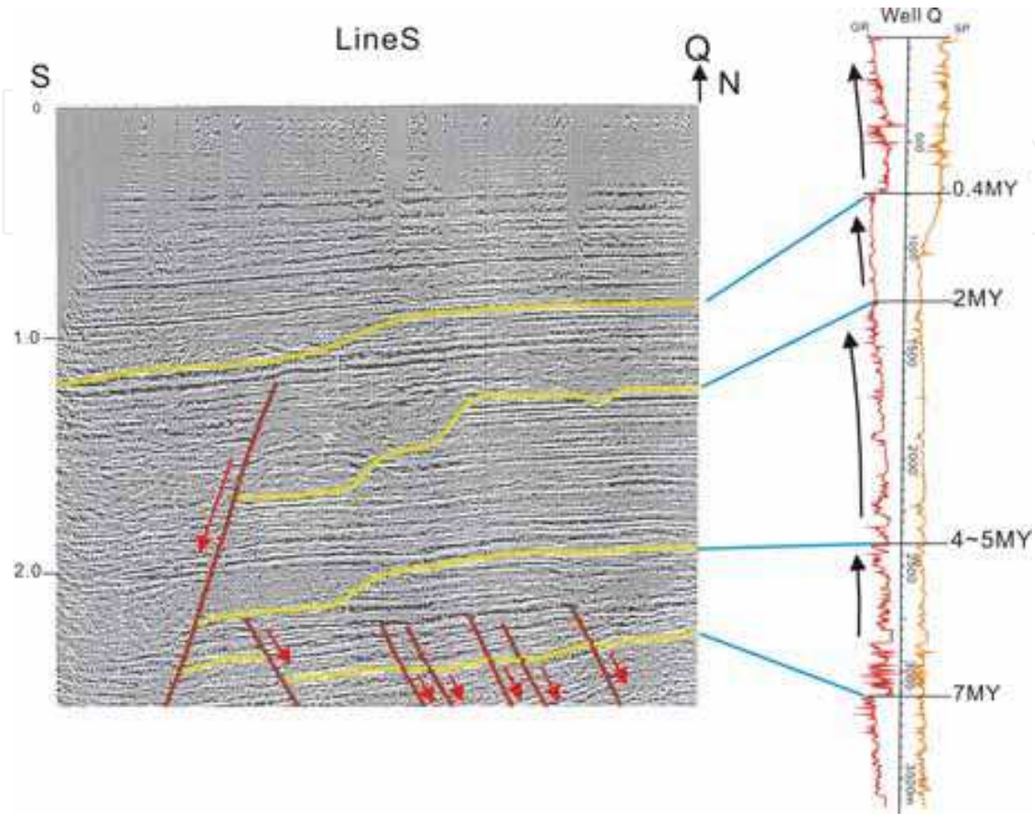

Fig. 9. Sedimentary cycles revealed by electric log data from well Q and their correlated sequences in the interpreted seismic line S. The sedimentary cycles are characterized by coarsening-upward sequences and are based by small-scaled unconformities, which turn into large-scaled down-cutting morphology of submarine canyons to the south.

5.3 Eustatic effects on stratigraphy architecture

A previous study of sequence stratigraphy of an outcropped section in the foothills belt [101] recognized several unconformities, including the one coeval with that of 2 My in the coastal plain, and suggested that the unconformities are the results of eustatic sea level fluctuation. In order to clarify the effect of eustasy on sedimentation of the foreland basin sequences in our study area, we compare the onset ages of rapid subsidence to the sea level fluctuation curves. The comparison demonstrates that the strata overlying the unconformities were deposited during the periods of sea level high stand or falling stage (Figure 10); the stratigraphy development is out-of-phase to the eustatic cycles. Therefore, the stratigraphic features in the foreland basin cannot be explained by eustatic sea-level fluctuation. Since the distribution of the strata directly overlying the unconformities is ubiquitous and not affected by the normal faults we suggest that such out-of-phase events should be related to subsidence induced by the telescopic effect of tectonic loading.

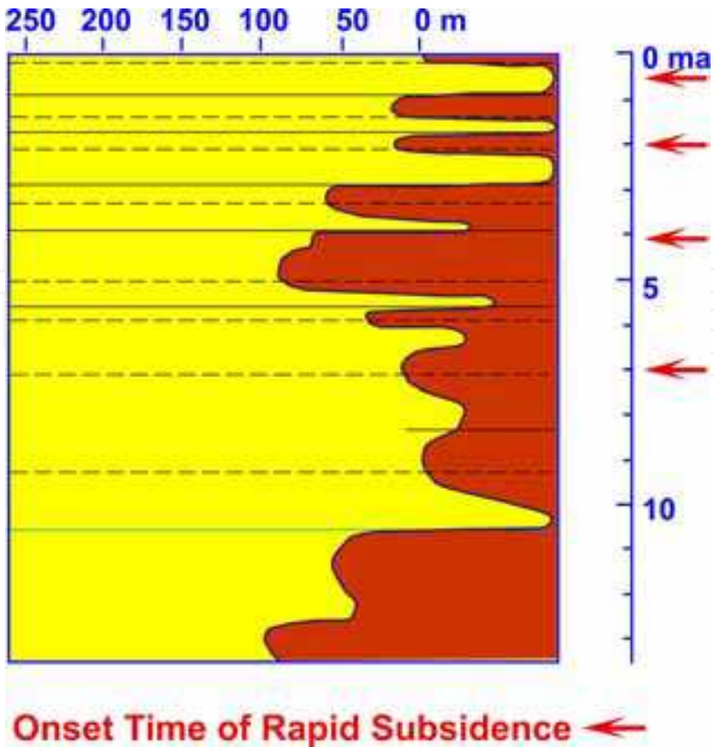

Fig. 10. Comparison of ages of rapid subsidence initiation to the eustatic sea level fluctuation [95] since the Late Miocene. All the rapid subsidence recorded in the foreland basin sequences happened in the sea level high stand or falling stages.

5.4 Tectonostratigraphic model for basin evolution

We have ruled out the possibility of eustatic effects on the stratigraphic architecture in the distal part of foreland basin. We suggest that the stratigraphic architecture, which is mainly shaped by the major unconformities, implies eastward migration of forebulge during episodic westward movement of the fold-and-thrust belt and later progradation of deposition toward the craton. Here, we propose a tectonostratigraphic model for the basin evolution in southwestern Taiwan since the beginning of latest extensional tectonics and through the foreland basin development.

The study area had been in the uplifted margin of the latest rifted basin up to 7 My bp (Figure 11a). The area encountered major normal faulting from 7 My bp to 4 My bp and syn-rift deposits were accumulated in downthrown side of the normal faults (Figure 11b), causing irregular spatial distribution of the stratal units of NN11-13 in the basin margin (Figures 7a and 8b). By the end of NN13 or at 5 to 4My bp, second phase of uplifting began (Figure 11c) and was followed by rapid subsidence and deposition of the ubiquitous strata of NN14 and the overlying strata onlapping toward the craton (Figure 11d). By the end of NN18 or at 2 My bp, the third phase of uplifting began, caused part of strata of NN14 and the overlying strata to be eroded (Figure 11e). From 2 My bp on, the uplifted area started to subside again and received another unit of ubiquitous strata of NN19 (Figure 11f.). The eroded area during the third phase of uplifting at 2 My bp, which boundary is defined by the transition between the unconformity and its correlated conformity, migrated cratonward relative to that of the preceding one.

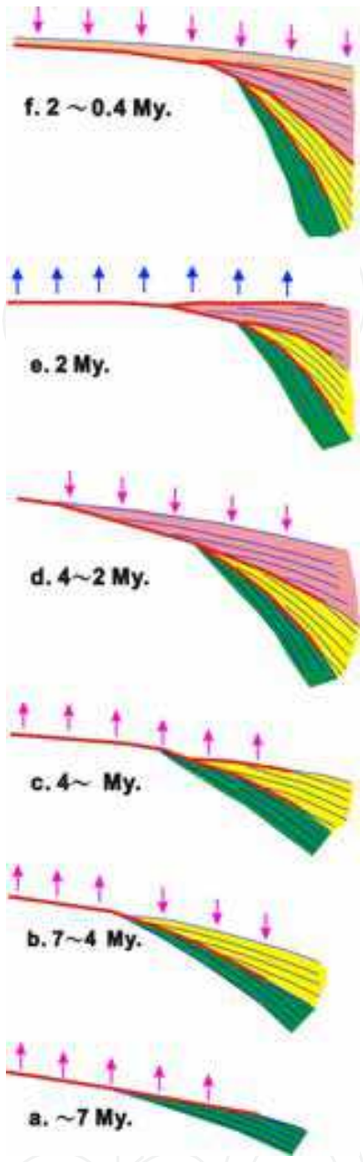

Fig. 11. Tectonostratigraphic model for the foreland basin evolution in southwestern Taiwan since the beginning of latest extensional tectonics and through the foreland basin development. Detailed descriptions for each stage are given in the text.

5.5 Tectonic implications

The characteristics of the subsidence history and stratigraphy architecture strongly imply that the foreland basin evolution favors the tectonostratigraphic model proposed by Flemings and Jordan [40] and Jordan and Flemings [41]. In their models, unconformity within the foreland basin sequences might represent active thrusting in the mountain-building belt, during which forebulge migrates toward the thrust front and causes uplifting in the distal part of the basin, while the rapid subsidence represents the later stage and quiescence of thrusting, during which sequences prograde toward the distal part of the basin and onto the unconformity. In southwestern Taiwan, sedimentation of the ubiquitous

stratal units of NN14 and NN19 may represent the quiescent period of active thrusting in the mountain-building belt.

Migration rate of the forebulge in the distal part of the foreland basin can be approximately measured based on the eastern limit of each unconformity and the western limit of each westward onlapping sequences (Figure 12). The back-and-forth variation in positions of the above stratigraphic settings would provide some significant clues to infer the kinematics of recent orogen-foreland basin development. The result indicates that the migration rate was slower in the early stage but higher in the final stage than that derived from the previously proposed kinematic model of steady migration of the orogenic belt [57]. This implies that the pre-collision extensional tectonics might have caused weaker lithosphere beneath the foreland basin and that once the foreland basin migrated onto the less stretched lithosphere the basin would expand rapidly into the craton.

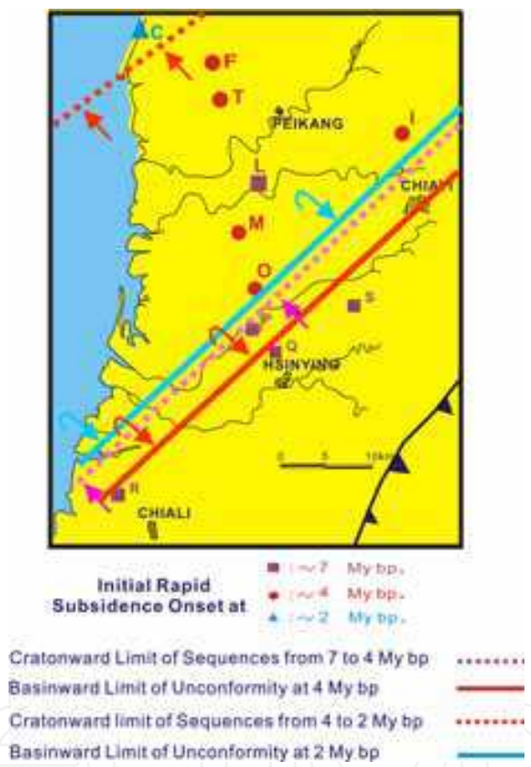

Fig. 12. Positions of the transition between the unconformities and their correlated conformities and the cratonward limitation of the distribution of unconformity-bounded sequences. The positions are determined based on the stratigraphy cross-sections (Figures 6a and 7a). Discussions of tectonic implication of variation in the positions are given in the text

6. Conclusions

1. Subsidence curves calculated from foreland basin sequences indicate that there are several rapid subsidence events at 7, 5 to 4, 2 and 0.2 My bp. The age of the initial rapid subsidence is younger toward the craton. The well sites that are characterized by earlier subsidence also record the other later events of rapid subsidence. Thus, the distal part of foreland basin encountered four discernible episodic events of rapid subsidence after the onset of rifting.

2. The stratigraphy cross-sections show that there are at least two unconformities in the foreland basin sequences, which divide the mega-sequence unit into several sequences of third-order scale. The characteristics of the unconformities are: 1, they merge into one unconformity toward the craton; 2, the time gap of each unconformity increases toward the craton, except where normal faulting created accommodation space for accumulation of older strata overlying the unconformity; 3, the spatial distribution of the younger unconformities with their correlated conformities shifts toward the craton.
3. Analysis of stratigraphy cross-sections indicates that the onset of foreland basin development was at 5 to 4 My bp, younger than that proposed in some previous studies.
4. The time-spatial distribution of the unconformities indicates back-and-forth migration of the basin margin in the distal part of foreland basin. The overlying sedimentary cycle of coarsening-upward sequences also implies the tectonic influence on the deposition of the foreland basin sequences in southwestern Taiwan.
5. The stratigraphic features in the foreland basin cannot be solely explained by eustatic sea-level fluctuation and the unconformities might result the episodic thrusting activity in the mountain-building belt to the east, which would cause eastward migration of forebulge and later progradation of deposition toward the craton.
6. The distal part of foreland basin in southwestern Taiwan had been in the uplifted margin of the latest rifted basin up to 7 My bp. The area encountered normal faulting from 7 My bp to 4 My bp. By the end of NN13 or at 5 to 4My bp, uplifting that corresponds to forebulge in the distal part of foreland basin began and was followed by rapid subsidence and deposition of the ubiquitous strata of NN14 and the overlying strata onlapping toward the craton. Close to 2 My bp, uplifting of the forebulge started again and caused part of strata of NN14 and the overlying strata to be eroded. From 2 My bp on, the uplifted area started to subside again and received another unit of ubiquitous strata of NN19.
7. The migration rate of the forebulge in the distal part of foreland basin was slower in the early stage than that derived from the previously proposed kinematic model for the steady migration of the orogenic belt. This implies that the pre-collision extensional tectonics might have caused weaker lithosphere beneath the foreland basin and that once the foreland basin migrated onto the less stretched lithosphere the basin would expand rapidly into the craton.

7. Acknowledgements

The authors like to thank Exploration and Development Research Institute, CPC Corporation, Taiwan, for providing invaluable well bore and seismic data and long-term supporting of the research works of this study. The authors thank Mr. Hsin-Hsiu Ting of Exploration and Development Research Institute, CPC Corporation, Taiwan, for reviewing and proof-reading the final manuscript. The authors also like to thank Ms. Yi-Jin Tang and Mr. Allen Zirei Yang from the Department of Earth Sciences, National Cheng Kung University, for preparing the figures and editing the text. Part of the research works of this study are the results of the project (NSC98-2116-M006-001) supported by National Science Council of Taiwan Government.

8. References

[1] DeCelles, P.G., and Giles, K.A., 1996. Foreland basin systems: Basin Research, 8: 105-123.
[2] Beaumount, C., 1981. Foreland basins: Geophysical Journal Royal Astronomical Society, 65: 291-329.

[3] Jordan, T.E., 1981. Thrust loads and foreland basin evolution, Cretaceous, Western United States: American Association of Petroleum Geologists Bulletin, 65: 2506-2520.

[4] Turcotte, D.L., and Schubert, G., 2002. Geodynamics (second edition). Cambridge University Press, Cambridge, 456 p.

[5] Shanmugam, G., and Walker, K.R., 1980. Sedimentation, subsidence, and evolution of foredeep basin in the Middle Ordovician, southern Appalachian: American Journal of Science, 180: 478-496.

[6] Heller, P.L., Bowdler, S.S., Chamber, H.P., Coogan, J.C., Hagan, E.S., Shuster, M.W. and Winslow, N.S., 1986. Time of initial thrusting in the Sevier orogenic belt, Idaho-Wyoming and Utah: Geology, 14: 388-391.

[7] Homewood, P., Allen, P.A. and Williams, G.D., 1986. Dynamics of the Molasse Basin of western Switzerland, in Allen, P.A., and Homewood, P., editors, Foreland Basins, Special Publication of the International Association of Sedimentologists, Blackwell Scientific Publication, Oxford, p. 199-218.

[8] Jordan, T.E., Flemings, P.B., and Beer, J.A., 1988. Dating thrust-fault activity by use of foreland basin strata, in Kleinspehn, K. L., and Paola, C., editors, New Perspectives in Basin Analysis, Springer-Verlag, New York, p. 307-330.

[9] Hayward, A.B., 1984. Sedimentation and basin formation related to ophiolite nappe emplacement, Miocene, SE. Turkey: Sedimentary Geology, 40: 105-191.

[10] Blair, T.C., and Bilodeau, W.L., 1988. Development of tectonic cyclothems in rift, pull-apart and foreland basins: Sedimentary response to episodic tectonism: Geology, 16: 517-520.

[11] Heller, P.L., Angevine, C.L. and Winslow, N. S., 1988. Two-phase stratigraphic model of foreland basin sequences: Geology, 16: 501-504.

[12] Allen, P.A., Homewood, P. and Williams, G.D., 1986. Foreland basin: An Introduction, in Allen, P. A., and Homewood, P., editors, Foreland Basin, Special Publication of the International Association of Sedimentologists, Blackwell Scientific Publication, Oxford, p. 3-12.

[13] Kleinspehn, P.B. and Poala, C., 1988, New perspectives in basin analysis, Springer-Verlag, New York, 453 p.

[14] Jacobi, R.D., 1981. Peripheral bulge-A causal mechanism for the Lower/ Middle Ordovician unconformity along the western margin of the Northern Appalachian: Earth and Planet Science Letters, 56: 245-251.

[15] Speed, R.C., and Sleep, N.H., 1982. Antler orogeny and foreland basin: A model: Geological Society of American Bulletin, 93: 815-828.

[16] Mussman, W.J., and Read J.F., 1986. Sedimentology and development of a passive- to convergent-margin unconformity: Middle Ordovician Knox unconformity, Virginia Appalachians: Geological Society of American Bulletin, 97: 282-295.

[17] Cohen, C.R., 1982. Model for a passive to active continental margin transition: Implications for hydrocarbon exploration: American Association of Petroleum Geologists Bulletin, 66: 708-718.

[18] White, T., Furlong, K., and Arthur, M., 2002. Forebulge migration in the Cretaceous Western Interior basin of the central United States: Basin Research, 14: 43-54.

[19] Allen, P.A., and Allen, J.R., 1990. Basin Analysis: Principles and Applications, Blackwell Scientific Publication, 451 p.

[20] Allen, P.A., and Allen, J.R., 2005. Basin Analysis: Principles and Applications (second edition), Blackwell Scientific Publication, 560 p.

[21] Sinclair, H.D., Coakley, B.J, Allen, P.A. and Watts, A.B., 1991. Simulation of foreland basin stratigraphy using a diffusion model of mountain belt uplift and erosion: An example from the central Alps, Switzerland: Tectonics, 10: 599-620.

[22] Crampton, S.L., and Allen, P.A., 1995. Recognition of forebulge unconformities associated with early stage foreland basin development: Example from the North Alpine Foreland Basin: American Association of Petroleum Geologists Bulletin, 79: 1495-1514

[23] Yu, H.S., and Chou, Y.W., 2001. Characteristics and development of the flexural forebulge and basal unconformity of Western Taiwan Foreland Basin: Tectonophysics, 333: 277-291.

[24] Quinlan, G.M., and Beaumont, C., 1984. Appalachian thrusting, lithospheric flexure, and the Paleozoic stratigraphy of the Eastern Interior of North America: Canadian Journal of Earth Science, 21: 973-996.

[25] Tankard, A.J, 1986. On the depositional response to thrusting and lithospheric flexure: Examples from the Appalachian and Rocky Mountain basins, in Allen, P. A., and Homewood, P., editors, Foreland Basins, Special Publication of the International Association of Sedimentologists, Blackwell Scientific Publication, p. 369-392.

[26] Royden, L.H., Patacca, E., and Scandone, P., 1987. Segmentation and configuration of subducted lithosphere in Italy: An important control on thrust-belt and foredeep-basin evolution: Geology, 15: 714-717.

[27] Karner, G.D., and Watts, A.B., 1983. Gravity anomalies and flexure of the lithosphere at mountain ranges: Journal of Geophysical Research, 88: 10449-10477.

[28] Lyon-Caen, H., and Molnar, P., 1983. Constraints on the structure of the Himalayas from an analysis of gravity anomalies and a flexural model of the lithosphere: Journal of Geophysical Research, 88: 8171-8191.

[29] Wu, P., 1991. Flexure of lithosphere beneath the Alberta foreland basin: Evidence of an eastward stiffening continental lithosphere: Geophysical Research Letter, 18: 451-454.

[30] Waschbusch, P.J, and Royden, L.H., 1992. Episodicity in foredeep basins: Geology, 20: 915-918.

[31] Beaumont, C., Keen, C.E., and Boutilier, R., 1982. A Comparison of Foreland and Rift Margin Sedimentary Basins: Philosophical Transactions of the Royal Society of London Series a-Mathematical Physical and Engineering Sciences, 305: 295-317.

[32] Stockmal, G.S., Beaumont, C. and Boutilier, R., 1986. Geodynamic models of convergent tectonics: the transition from rifted margin to overthrust belt and consequences for foreland-basin development: American Association of Petroleum Geologists Bulletin, 70: 181-190.

[33] Watts, A.B., 1992. The effective elastic thickness of the lithosphere and the evolution of foreland basins: Basin Research, 4: 169-178.

[34] Lehmann, D., Brett, C.E., Cole, R. and Baird, G., 1995. Distal sedimentation in a peripheral foreland basin: Ordovician black shales and associated flysch of the western Taconic foreland, New York State and Ontario: Geological Society of American Bulletin, 107: 708-724.

[35] Lihou, J.C., and Allen, P.A., 1996. Importance of inherited rift margin structures in the early North Alpine Foreland Basin, Switzerland: Basin Research, 8: 425-442.

[36] Gupta, S., and Allen, P.A., 2000. Implications of foreland paleotopography for stratigraphic development in the Eocene distal Alpine foreland basin: Geological Society of American Bulletin, 112: 515-530.

[37] Bayona, G., and Thomas, W.A., 2003. Distinguishing fault reactivation from flexural deformation in the distal stratigraphy of the Peripheral Blountian Foreland Basin, southern Appalachians, USA: Basin Research, 15:503-526.

[38] Blair, T.C., and Bilodeau, W.L., 1988. Development of tectonic cyclothems in rift, pull-apart and foreland basins: Sedimentary response to episodic tectonism: Geology, 16: 517-520.

[39] Flemings, P.B., and Jordan, T.E., 1989. A synthetic stratigraphic model of foreland basin development: Journal of Geophysical Research, 94: 3851-3866.

[40] Flemings, P.B., and Jordan, T.E., 1990. Stratigraphic modeling of foreland basins: Interpreting thrust deformation and lithosphere rheology: Geology, 18: 430-434.

[41] Jordan, T.E., and Flemings, P.B., 1991. Large-scale stratigraphic architecture, eustatic variation, and unsteady tectonism: A theoretical evaluation: Journal Geophysical Research, 96: 6681-6699.

[42] Johnson, D.D., and Beaumont, C., 1995. Preliminary results from a planform kinematic model of orogeny evolution, surface processes and the development of clastic foreland basin stratigraphy, in Dorobek, S.L., and Ross, G.M, editors, Stratigraphic Evolution of Foreland Basin: *Society of Economic Paleontologists* and Mineralogists *Special Publication,* 52: 3-24.

[43] Jordan, T.E., 1995. Retroarc foreland and related basins, in Busby, C. J., and Ingersoll, R. V., editors, Tectonics of Sedimentary Basins, Blackwell Science, Cambridge, p. 331-362.

[44] Catuneanu, O., Beaumont, C. and Waschbusch, P., 1997. Interplay of static loads and subduction dynamics in foreland basins: Reciprocal stratigraphies and the "missing" peripheral bulge: Geology, 25: 1087-1090.

[45] Catuneanu, O., Hancox, P.J and Rubidge, B.S., 1998. Reciprocal flexural behaviour and contrasting stratigraphies: A new basin development model for the Karoo retroarc foreland system, South Africa: Basin Research, 10: 417-439.

[46] Galewsky, J., 1998. The dynamics of foreland basin carbonate platforms: Tectonic and eustatic controls: Basin Research, 10: 409-416.

[47] Yong, L., Allen, P.A., Densmore, A.L. and Qiang, X., 2003. Evolution of the Longmen Shan foreland basin (western Sichuan, China) during the Late Triassic Indosinian Orogeny: Basin Research, 15: 117-138.

[48] Bayona, G., Cortes, M., Jaramillo, C., Ojeda, G., Aristizabal, J.J. and Reyes-Harker, A., 2008. An integrated analysis of an orogen-sedimentary basin pair: Latest Cretaceous-Cenozoic evolution of the linked Eastern Cordillera orogen and the Llanos foreland basin of Colombia: Geological Society of American Bulletin, 120: 1171-1197.

[49] Chou, Y.W., and Yu, H.S., 2002. Structural expressions of flexural extension in the arc-continent collisional foredeep of western Taiwan, in Byrne, T. B., and Liu, C. S., editors, Geology and geophysics of an arc-continent collision, Taiwan: Geological Society of America Special Papers, 358: 1-12.

[50] Lin, A.T., and Watts, A.B., 2002. Origin of the West Taiwan basin by orogenic loading and flexure of a rifted continental margin: Journal Geophysical Research, 107: 2-19.
[51] Lin, A.T., Watts, A.B. and Hesselbo, S.P., 2003. Cenozoic stratigraphy and subsidence history of the South China Sea margin in the Taiwan region: Basin Research, 15: 453-478.
[52] Yang, K.M., Huang, S.T., Wu, J.C., Ting, H.H. and Mei, W.W., 2006. Review and new insights on foreland tectonics in western Taiwan: International Geology Review, 48: 910-941.
[53] Covey, M., 1984. Lithofacies analysis and basin reconstruction, Plio-Pleistocene western Taiwan foredeep: Petroleum Geology of Taiwan, 20: 53-83.
[54] Covey, M., 1986. The evolution of foreland basins to steady state: evidence from the Western Taiwan foreland basin, in Allen, P., and Homewood, P., editors, Foreland Basins, Special Publications of the International Association Sedimentologists, 8: 77-90.
[55] Yang, K.M., Wu, J.C., and Chi, W.R., 1994. The tectonic implication of stratigraphy in the foreland basin: Program with abstracts, 1994 annual meetng, Geological Society of China, Taipei, p. 103-107.
[56] Chi, W.R., Yang, K.M., Wu, J.C., Chen, H.M., and Tang, H.M. 1987. The application of backstripping method in basin analysis and oil exploration of the Peikang area, Bulletin of Exploration and Development Research, 10: 63-88 (*in Chinese*).
[57] Suppe, J, 1981. Mechanics of mountain building and metamorphisms in Taiwan. *Memoir* of the *Geological Society of China*, 4: 67-89.
[58] Yang, K.M., Wu, J.C., Chi, W.R., and Ting, H.H., 2000. The tectonic implication of stratigraphy architecture in the foreland basin, western Taiwan (abstracts): American Association of Petroleum Geology 2000 Annual Convention, A162.
[59] Biq, C.C., 1972. Dual-trench structure in the Taiwan-Luzon region: Proceedings of the Geological Society of China, 15: 65-75.
[60] Chai, B.H.T., 1972. Structure and tectonic evolution of Taiwan: American Journal Science, 272: 389-422.
[61] Tsai, Y.B., 1978. Plate subduction and the Plio-Pleistocene orogeny in Taiwan: Petrology Geology of Taiwan, 15: 1-10.
[62] Teng, L.S. and Wang, Y., 1981. Island arc system of the Coastal Range, eastern Taiwan: Proceedings of the Geological Society of China, 24: 99-112.
[63] Suppe, J., 1984. Seismic interpretation of the compressively reactivated normal fault near Hsinchu, western Taiwan: Petroleum Geology of Taiwan, 20: 85-96.
[64] Chi, W.R., Namson, J., and Suppe, J., 1981. Record of plate interactions in the Coastal Range, Eastern Taiwan: *Memoir* of the *Geological Society of China*, 4: 155-194.
[65] Chou, J.T., 1973. Sedimentology and paleontology of the Upper Cenozoic system of Wewstern Taiwan: Proceedings of the Geological Society of China, 16: 111-143.
[66] Teng, L.S., 1987. Stratigraphic records of the Late Cenozoic Penlai Orogeny of Taiwan: Acta Geologica Taiwanica, 25: 205-224.
[67] Teng, L.S., 1990. Geotectonic evolution of late Cenozoic arc-continent collision in Taiwan: Tectonophysics, 183: 57-76.
[68] Huang, C.Y., Wu, W.Y., Chang C.P., Tsao, S., Yuan, P.B., Lin C.W. and Kuan-Yuan, X., 1997. Tectonic evolution of accretionary prism in the arc-continent collision terrane of Taiwan: Tectonophysics, 281: 31-51.

[69] Huang, C.Y., Yuan, P.B. and Tsao, S.J, 2006. Temporal and spatial records of active arc-continent collision in Taiwan: A synthesis: Geological Society of American Bulletin, 118: 274-288.

[70] Sun, S.C., 1982. The Tertiary basins of offshore Taiwan: Proceedings of the Second ASCOPT Conference and Exhibition, Manila, Philippine, p. 126-135.

[71] Yuan, J, Chen, J.T., Chow, C.T., Yang, K.M., Chen, H.M. and Lo, H.R., 1989. Evolution of Tertiary basins of western Taiwan and appraisal of hydrocarbon potentialities-Northern Basin and Peikang High region: Unpublished Report, CPC, MOEA, R.O.C. (*in Chinese*).

[72] Ru, K., and Pigott, J.D., 1986. Episodic Rifting and Subsidence in the South China Sea: American Association of Petroleum Geology, 70: 1136-1155.

[73] Hsiao, P.T., 1974. Subsurface geologic study of the Hsinying Coastal area, Taiwan: Petroleum Geology of Taiwan, 11: 27-39.

[74] Tang, C.H., 1977. Late Miocene erosional unconformity on the subsurface Peikang high beneath the Chiayi-Yunlin Coastal Plain, Taiwan: *Memoir* of the *Geological Society of China*, 2: 155-167.

[75] Leu, R.T., Chiang, C.L. and Huang, F.W.F., 1985. Study on the Pachangchi structure, Chaiyi, Taiwan: Petroleum Geology of Taiwan, 21: 13-32.

[76] Chow, J., Yuan, J., and Yang, K.M., 1986. Geological interpretation of the seismic in the Houpi area, Taiwan: Petroleum Geology of Taiwan, 22: 27-53.

[77] Chow, J, Yang, K.M., and Chen, H.M., 1987. Structural traps of the Paiho area, Southern Taiwan: Petroleum Geology of Taiwan, 23: 13-39.

[78] Chow, J, Yang, K.M., and Chen, H.M., 1988, Seismic Interpretation of the Subsurface Structures in the Yichu-Chiali Area, Southern Taiwan: Petroleum Geology of Taiwan, 24: 60-95.

[79] Yuan, J, Yang, K.M., Chi, W.R., Hu, C.C., and Chou, T.F., 1988. Episodic tectonism in the Tertiary continental margin of western Taiwan (abstracts): International symposium of Geodynamic evolution of eastern Eurasian margin, Paris, France.

[80] Yang, K.M., Ting, H.H., and Yuan, J, 1991. Structural styles and tectonic modes of Neogene extensional tectonics in southwestern Taiwan: Implications for hydrocarbon exploration: Petroleum Geology of Taiwan, 26: 1-31.

[81] Wernicke, B., 1985. Uniform-sense normal simple shear of the continental lithosphere: Canadian Journal Earth Science, 22: 8-125.

[82] Isller, D., McQueen, H., and Beaumont, C., 1989. Thermal and isostatic consequences of simple shear extension of the continental lithosphere: Earth and Planet Science Letters, 91: 341-358.

[83] Lee, T.Y., Tang, C.H., Ting, J.S., and Hsu, Y.Y, 1993. Sequence stratigraphy of the Tainan Basin, offshore southwestern Taiwan: Petroleum Geology of Taiwan, 28: 119-158.

[84] Sun, S.C., 1985. The Cenozoic tectonic evolution of offshore Taiwan: Energy, v. 10, p. 421-432.

[85] Shiao, T.W., and Teng, L.S., 1991. Flexural tectonics of Western Taiwan Foreland Basin: A preliminary study: Proceeding of the Third Taiwan Symposium on Geophysics, p. 437-446.

[86] Chou, Y.W., 1999. Tectonic framework, flexural uplift history and structural patterns of flexural extension in Western Taiwan Foreland Basin. Ph.D. dissertation, Taipei, National Taiwan University, 125 p (*in Chinese*).

[87] DeCelles, P.G., and Giles, K.A., 1996. Foreland basin systems: Basin Research, 8: 105-123.
[88] Chou, S.C., Teng, L.S., Chung, H.S., and Shiao, T.W., 1994. Geohistory of West Taiwan Foreland Basin: A preliminary study: Petroleum Geology of Taiwan, 29: 289-322 (*in Chinese*).
[89] Simoes, M., and Avouac, J.P., 2006. Investigating the kinematics of mountain building in Taiwan from the spatiotemporal evolution of the foreland basin and western foothills: Journal of Geophysical Research, 111: B10401.
[90] Shaw, C.L., 1996. Stratigraphic correlation and isopach maps of the wetsern Taiwan: TAO, 7: 333-359.
[91] Tensi, J., Mouthereau, F. and Lacomb, O., 2006, Lithospheric bulge in the West Taiwan Basin: Basin Research, 18: 277-299.
[92] Watts, A.B., and Ryan, W.B.F., 1976. Flexure of the lithosphere and continental margin basins, Tectonophysics, 36: 25-44.
[93] Sclater, J., and Christie, P.A.F., 1980. Continental stretching: An explanation of the post-mid Cretaceous subsidence of the central North Sea basin: Journal of Geophysical Research, 85: 3771-3739.
[94] Okada, H., and Bukry, D., 1980. Supplementary modficaton and introduction of code numbers to the low-latitude coccolth biostratigraphic zonation: Marine Paleontology, 5: 321-325.
[95] Haq, B.U., Hardonbol, J, Vail, P.R., 1988. Mesozoic and Cenozoic chronostratigraphy and cycles of sea-level change, in Wilgus, C.K., Ross, C.A., and Posamentier, H., editors, Sea-Level changes: an integrated approach: Society of Economic Paleontologists and Mineralogists, Special Publication, 42: 71-108.
[96] Wu, J.C., Wang, M.H., Tsai, C.C., Chi, W.R., Mei., W.W., 1994. Analysis and correlation of biostratigraphy, paleosedimentary environment in Hsinying, Tainan: Bulletin of Expoloration and Development Research, 26: 381-394 (*in Chinese*).
[97] Yeh, M.G., and Yang, C.Y., 1994, Depositional Environments of the Upper Miocene Area, Chaiyi, Taiwan: Petroleum Geolology of Taiwan, 29: 193-224.
[98] Fuh, S.C., 2000. Magnitude of Cenozoic erosion from mean sonic transit time, offshore Taiwan: Marine Petroleum Geology, 17: 1011-1028.
[99] Fuh, S.C., Liang, S.C., and Wu, M.S., 2003. Spatial and Temporal Evolution of the Plio-Pleistocene Submarine Canyons between Potzu and Tainan, Taiwan: Petroleum Geology of Taiwan, 36: 1-18.
[100] Fuh, S.C., Chern, C.C., Liang, S.C., Yang. Y.L., Wu, S.H., Chang T.Y. and Lin J.Y., 2009. The biogenic Gas Potential of the submarine canyon systems of Plio-Pleistocene foreland basin, southwestern Taiwan: Marine Petroleum Geology, 26: 1087-1099.
[101] Chen, W.S., Ridgway, K.D., Horng, C.S., Chen, Y.G., Shea, K.S. and Yeh, M.G., 2001. Stratigraphic architecture, magnetostratigraphy, and incised-valley systems of the Pliocene-Pleistocene collisional marine foreland basin of Taiwan: Geological Society of American Bulletin, 113: 1249-1271.

Tectonics
Edited by Dr. Damien Closson

ISBN 978-953-307-545-7
Hard cover, 358 pages
Publisher InTech
Published online 28, February, 2011
Published in print edition February, 2011

The term tectonics refers to the study dealing with the forces and displacements that have operated to create structures within the lithosphere. The deformations affecting the Earth's crust are result of the release and the redistribution of energy from Earth's core. The concept of plate tectonics is the chief working principle. Tectonics has application to lunar and planetary studies, whether or not those bodies have active tectonic plate systems. Petroleum and mineral prospecting uses this branch of knowledge as guide. The present book is restricted to the structure and evolution of the terrestrial lithosphere with dominant emphasis on the continents. Thirteen original scientific contributions highlight most recent developments in seven relevant domains: Gondwana history, the tectonics of Europe and the Near East; the tectonics of Siberia; the tectonics of China and its neighbourhood; advanced concepts on plate tectonics are discussed in two articles; in the frame of neotectonics, two investigation techniques are examined; finally, the relation between tectonics and petroleum researches is illustrated in one chapter.

InTech Europe
University Campus STeP Ri
Slavka Krautzeka 83/A
51000 Rijeka, Croatia
Phone: +385 (51) 770 447
Fax: +385 (51) 686 166
www.intechopen.com

InTech China
Unit 405, Office Block, Hotel Equatorial Shanghai
No.65, Yan An Road (West), Shanghai, 200040, China
中国上海市延安西路65号上海国际贵都大饭店办公楼405单元
Phone: +86-21-62489820
Fax: +86-21-62489821

IntechOpen